Biochemistry and Biophysics Reports 10 (2017) 137–144

Contents lists available at ScienceDirect

Biochemistry and Biophysics Reports

journal homepage: www.elsevier.com/locate/bbrep

Dual role of imidazole as activator/inhibitor of sweet almond (*Prunus dulcis*) β-glucosidase

Sara Caramia[a], Angela Gala Morena Gatius[a], Fabrizio dal Piaz[b], Denis Gaja[a], Alejandro Hochkoeppler[a,c,*]

[a] Department of Pharmacy and Biotechnology, University of Bologna, Viale Risorgimento 4, 40136 Bologna, Italy
[b] Department of Medicine, University of Salerno, Via Giovanni Paolo II 132, 84084 Fisciano, SA, Italy
[c] CSGI, University of Firenze, Via della Lastruccia 3, 50019 Sesto Fiorentino, FI, Italy

ARTICLE INFO

Keywords:
β-glucosidase
Sweet almond
Prunus dulcis
Imidazole

ABSTRACT

The activity of *Prunus dulcis* (sweet almond) β-glucosidase at the expense of *p*-nitrophenyl-β-D-glucopyranoside at pH 6 was determined, both under steady-state and pre-steady-state conditions. Using crude enzyme preparations, competitive inhibition by 1–5 mM imidazole was observed under both kinetic conditions tested. However, when imidazole was added to reaction mixtures at 0.125–0.250 mM, we detected a significant enzyme activation. To further inspect this effect exerted by imidazole, β-glucosidase was purified to homogeneity. Two enzyme isoforms were isolated, i.e. a full-length monomer, and a dimer containing a full-length and a truncated subunit. Dimeric β-glucosidase was found to perform much better than the monomeric enzyme, independently of the kinetic conditions used to assay enzyme activity. In addition, the sensitivity towards imidazole was found to differ between the two isoforms. While monomeric enzyme was indeed found to be relatively insensitive to imidazole, dimeric β-glucosidase was observed to be significantly activated by 0.125–0.250 mM imidazole under pre-steady-state conditions. Further, steady-state assays revealed that the addition of 0.125 mM imidazole to reaction mixtures increases the K_m of dimeric enzyme from 2.3 to 6.7 mM. The activation of β-glucosidase dimer by imidazole is proposed to be exerted via a conformational transition poising the enzyme towards proficient catalysis.

1. Introduction

According to their catalytic mechanism, β-glucosidases are classified as inverting or retaining glycohydrolases [1–3]. Remarkably, inverting and retaining β-glucosidases share, along their reaction paths, the generation of a transition state characterized by sp^2 hybridization of the glucose C1 [4]. Accordingly, the planar nature of glucose C1 in the transition state is of importance to design enzyme inhibitors.

To date, quite a number of β-glycohydrolases were characterized and classified into different families according to their primary structures. Sweet almond (*Prunus dulcis*) β-glucosidase (EC 3.2.1.21) contains the sequence motif ITENG, which includes a catalytic glutamate (E426), and is diagnostic of family 1 enzymes [5]. This enzyme was shown to feature broad specificity [6,7], and to act according to a retaining mechanism [8]. Moreover, it was recently demonstrated that the two catalytic steps, respectively leading to glycosilated enzyme and to the release of glucose, feature SN2 and SN1 character, respectively [9]. The pH-dependence of sweet almond β-glucosidase activity is bell-shaped [7,10], suggesting the titration of the two acidic residues involved in catalysis. The pH optimum is centered at 5.6 [10,11], and the two pKa values accordingly determined are equal to 4.4 and 6.7 [7,10]. These values can be reasonably assigned to the nucleophile (E426) and to the acid/base catalytic residue, respectively. Interestingly, a detailed and elegant inspection of the effects, if any, of ionic strength on the sweet almond enzyme revealed that both NaCl and LiCl decrease and increase the acidity of E426 and of the acid/base catalytic residue, respectively [12]. In particular, the decrease of E426 pKa induced by ionic strength suggests a non trivial effect, e.g. that the two catalytic residues interact and mutually affect their acid/base properties [12].

The broad specificity of sweet almond β-glucosidase is easily explained by the rather small differences between the k_{cat}/K_m second-order rate constants observed in the presence of *p*-nitrophenyl derivatives of fucose, glucose, and galactose [7]. The same poor specificity holds when the aglycone is considered: about 20 different derivatives of glucose were shown to be susceptible of cleavage by the sweet almond

* Corresponding author at: Department of Pharmacy and Biotechnology, University of Bologna, Viale Risorgimento 4, 40136 Bologna, Italy.
E-mail address: a.hochkoeppler@unibo.it (A. Hochkoeppler).

http://dx.doi.org/10.1016/j.bbrep.2017.03.007
Received 28 November 2016; Received in revised form 14 March 2017; Accepted 23 March 2017
Available online 24 March 2017

enzyme. However, in this case the k_{cat}/K_m ratio varies over three orders of magnitude, depending on the pKa of the aglycone leaving group, the best substrates being those with the lower pKa [7,13].

The finding that some defects of β-glucosidases are linked to human diseases, e.g. the Gaucher syndrome [14], prompted detailed investigations on compounds able to inhibit these enzymes. Early enough, a vast array of potential inhibitors of sweet almond β-glucosidase was tested [7]. In particular, different carbohydrates, lactones, phenols and amines, comprising quite a number of their derivatives, were assayed. Amines and lactones were more effective as inhibitors when compared to carbohydrates and phenols [7]. Later on, imidazole, as well as histidine, histamine, and histidinol [15,16] were found to be potent inhibitors of sweet almond β-glucosidase, with K_i values ranging from 1 to 7 μM (histidinol, histamine, and histidine) to 0.5 mM (imidazole). The action of these compounds as proton buffers, therefore interfering with catalysis, was proposed [16].

Despite the detailed knowledge accumulated on sweet almond β-glucosidase, some relevant points concerning this enzyme were not elucidated yet. In particular, the tertiary structure is not known, and the contribution to observed enzyme kinetics by monomeric and oligomeric forms was not investigated. The primary structure of sweet almond β-glucosidase contains 544 amino acids, yielding a molecular mass equal to 62 kDa. Previous studies have described the native enzyme as a dimer, but the search for activity by a monomeric form was never attempted. Moreover, it was observed that some potent inhibitors of sweet almond β-glucosidase, e.g. nojirimycin, do not trigger linear effects as a function of their concentration. This was explained by conformational changes of the enzyme induced by inhibitor binding [17], similarly to what proposed for substrate binding [18]. To deepen the knowledge about sweet almond β-glucosidase, and the mode of action of enzyme inhibitors, we report here on the activity of crude and highly purified enzyme isoforms. In particular, the kinetics of the reaction at the expense of *p*-nitrophenyl-β-D-glucopyranoside is shown, both under steady-state and pre-steady-state conditions, in the absence or in the presence of imidazole.

2. Materials and methods

2.1. Materials

Lyophilized β-glucosidase from sweet almonds, buffers, and *p*-nitrophenyl-β-D-glucopyranoside (PNPGluc) were obtained from Sigma-Aldrich (St. Louis, MO, USA). Pre-packed HiTrap-Q anion exchange column, and Superdex 200 resin were from GE Healthcare Life Sciences (Piscataway, NJ, USA). Electrophoresis reagents of high purity were purchased from Bio-Rad (Hercules, CA, USA).

2.2. Partial purification of β-glucosidase

The enzyme powder was dissolved in 50 mM Tris-HCl, 150 mM NaCl (pH 8), the solution was centrifuged (10,000 × *g*, 20 min), and the supernatant was loaded onto a Superdex 200 column (1.6 × 70 cm), previously conditioned with 50 mM Tris-HCl, 150 mM NaCl, pH 8. The flow rate was 0.6 mL/min, 0.9 mL fractions were collected, and then subjected to SDS-PAGE to detect the presence of dimeric and monomeric β-glucosidase.

2.3. Purification to homogeneity of β-glucosidase

The enzyme powder was dissolved in 50 mM Tris-HCl (pH 8), the solution was centrifuged (10,000 × *g*, 20 min), and the supernatant was loaded onto a HiTrap-Q (5 mL) column, conditioned with 50 mM Tris-HCl (pH 8). After loading the sample, the column was washed with the equilibration buffer (10 column volumes), and a linear 0–600 mM NaCl gradient was then applied. A consistent fraction of β-glucosidase was eluted with the column wash. This fraction was then concentrated and loaded onto a gel filtration Superdex 200 column (1.6 × 70 cm), previously conditioned with 50 mM Tris-HCl, 150 mM NaCl, pH 8. The flow rate was 0.6 mL/min, 0.9 mL fractions were collected, and then subjected to SDS-PAGE. The fractions containing pure monomeric or dimeric isoforms of β-glucosidase were concentrated with an Amicon ultrafiltration cell, equipped with a YM-30 membrane, and then stored at −20 °C until used. The gel filtration column was calibrated with Low-Molecular-Weight protein standards (GE Healthcare Life Sciences).

2.4. Steady-state activity assays

The activity of sweet almond β-glucosidase was assayed at 20 °C in a universal buffer containing 25 mM each of MES, MOPS, and Tris [19]. The release of *p*-nitrophenol at the expense of PNPGluc was determined spectrophotometrically at 347 nm, using a Cary 300 UV–VIS spectrophotometer. The molar extinction coefficient of *p*-nitrophenol at 347 nm was assumed equal to 3500 $M^{-1}cm^{-1}$ [7].

2.5. Stopped-flow experiments

All measurements were performed using a KinTek (Snow Shoe, PA, USA) SF2004 stopped-flow equipment, and detecting the release of *p*-nitrophenol from PNPGluc at 347 nm. The enzyme syringe contained crude or purified β-glucosidase (in universal buffer, pH 6) at the indicated concentrations, and the second syringe contained 1.1 mM pNPGluc dissolved in universal buffer, pH 6. When present, imidazole (dissolved in universal buffer, pH 6) was added to the enzyme syringe. All the assays were performed at 20 °C.

2.6. Protein assay

Protein concentration was determined according to Bradford [20].

2.7. Mass spectrometry

Elution of proteins from acrylamide gels, trypsin digestion, and separation of peptides were performed as previously described [21]. The resulting peptides were analyzed by LC-MS/MS using an Orbitrap XL instrument (Thermo Fisher, Waltham, MA, USA) equipped with a nano-ESI source coupled with a nano-Acquity capillary UPLC (Waters, Milford, MA, USA). Briefly, peptides were separated with a capillary BEH C18 column (0.075 × 100 mm, 1.7 μM, Waters) using aqueous 0.1% formic acid (A) and CH_3CN containing 0.1% formic acid (B) as mobile phases. Peptides were eluted by means of a linear gradient from 5% to 50% of B in 90 min, at a 300 nL/min flow rate. Mass spectra were acquired over an *m/z* range from 400 to 1800. To achieve protein identification, MS and MS/MS data underwent Mascot Search Engine software analysis to interrogate the National Center for Biotechnology Information nonredundant (NCBInr) protein database. Parameters sets were: trypsin cleavage; carbamidomethylation of cysteines as a fixed modification and methionine oxidation as a variable modification; a maximum of two missed cleavages; false discovery rate, calculated by searching the decoy database, 0.05.

3. Results

3.1. Steady-state assays with crude enzyme

As a first test, we assayed the activity of crude β-glucosidase towards *p*-nitrophenyl-β-D-glucopyranoside (pNPGluc) as a function of pH. To this aim, we dissolved the lyophilized enzyme powder in a universal buffer (composed of MES, MOPS, and Tris, 25 mM each) equilibrated at pH 5.5, 6, 6.25, 6.5, 6.75, 7, or 7.5. The enzyme aliquots accordingly prepared were then used to assay the activity, at each pH value considered, as a function of pNPGluc concentration (Fig. 1A and B). The apparent K_m and V_{max} were determined, and the decrease of

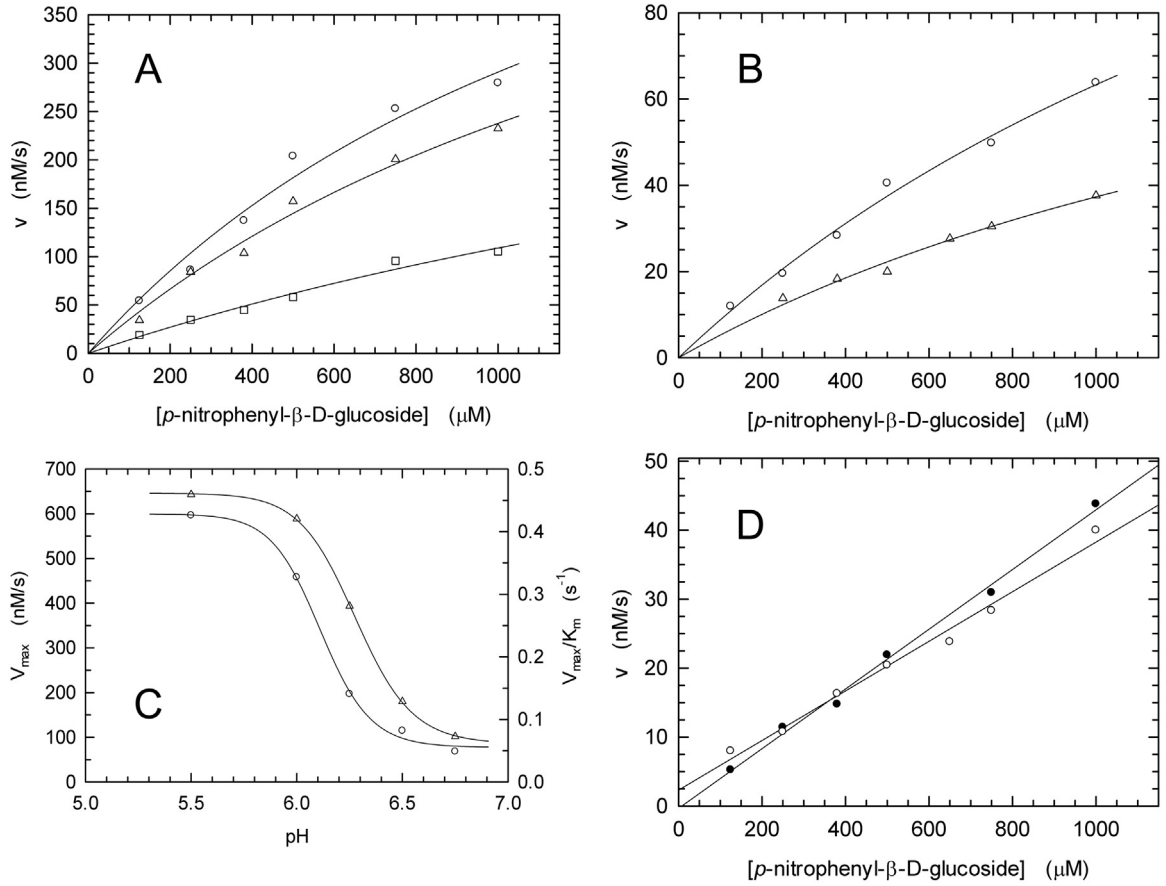

Fig. 1. Kinetics of reactions catalyzed by crude sweet almond β-glucosidase at the expense of *p*-nitrophenyl-β-D-glucopyranoside. (A) Initial reaction velocities detected as a function of substrate concentration in the presence of 60 μg/mL of crude enzyme at pH 5.5 (circles), 6 (triangles), or 6.25 (squares). (B) Initial reaction velocities detected at pH 6.5 (circles), or 6.75 (triangles). Other conditions as in Panel A. (C) Dependence of V_{max} (triangles) and V_{max}/K_m (circles) on pH. The catalytic constants were calculated from the data reported in Panels A and B. (D) Initial reaction velocities detected at pH 7.0 (open circles), or 7.5 (filled circles), in the presence of 0.3 mg/mL of crude enzyme.

both kinetic constants as a function of pH suggests the titration of a single catalytic residue, the pKa of which was estimated equal to 6.10 ± 0.03 or 6.28 ± 0.006, considering V_{max} or V_{max}/K_m, respectively (Fig. 1C). Interestingly, when activity assays were performed at pH 7 or 7.5, zero-order kinetics was not detected, and the initial velocity of the observed reactions did linearly increase as a function of PNPGluc concentration, up to 1 mM substrate (Fig. 1D). This suggests that the K_m of the enzyme does significantly increase upon titration of the catalytic residue featuring pKa equal to 6.1–6.3.

We then tested the effect of different imidazole concentrations towards β-glucosidase activity. These assays were performed at pH 6, using pNPGluc as substrate. Not surprisingly, when added to reaction mixtures at 1 or 5 mM, imidazole did inhibit enzyme activity (Fig. 2). Moreover, imidazole clearly acted, at these concentrations, as a competitive inhibitor (Fig. 2), raising the apparent K_m, and not altering V_{max} (Table 1). However, we unexpectedly observed a completely different behaviour when imidazole was used at 0.5 or 0.25 mM. In this case, not only K_m was affected, but V_{max} did also increase (Fig. 2, Table 1).

To further investigate the effect of imidazole towards β-glucosidase, we assayed enzyme activity at pH 6 under pre-steady-state conditions. To this aim, we used a stopped-flow, the two syringes of which were respectively filled with enzyme and 1.1 mM pNPGluc. In particular, the enzyme syringe was filled with β-glucosidase only or with enzyme and 0.25, 0.5, or 2.5 mM imidazole. Not surprisingly again, the higher concentration of imidazole did strongly inhibit enzyme activity (Fig. 3A). However, when the low concentrations of imidazole were assayed, we clearly observed a transient, but significant, initial activation of β-glucosidase (Fig. 3A and B). This activation was then followed

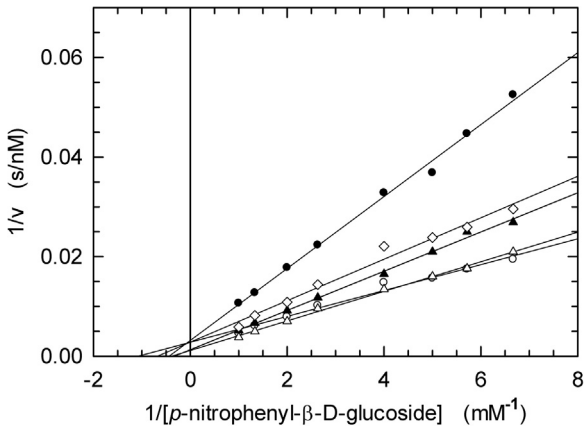

Fig. 2. Lineweaver-Burk plots of initial velocities of reactions catalyzed by sweet almond β-glucosidase. Assays were performed using 60 μg/mL of crude enzyme, in the absence (empty circles) or in the presence of 0.25 (empty triangles), 0.5 (filled triangles), 1 mM (empty diamonds), or 5 mM (filled circles) imidazole.

by inhibition of the enzyme, and the observed reaction velocities were slightly slower than the corresponding velocity detected in the absence of imidazole (Fig. 3B). Moreover, the activation effect triggered by imidazole was approximately proportional to concentration, and did consistently shorten the lag-phase observed in its absence before the onset of maximal activity (Fig. 3B).

Table 1
Sweet almond β-glucosidase kinetic constants determined assaying the activity of crude enzyme (60 μg/mL) in the presence or in the absence of imidazole and using *p*-nitrophenyl-β-D-glucopyranoside as substrate.

[Imidazole] (mM)	K_m (mM)	V_{max} (nM/s)
–	0.92 ± 0.05	353 ± 73
0.25	2.50 ± 0.06	846 ± 202
0.50	2.95 ± 0.08	748 ± 241
1.00	1.45 ± 0.08	350 ± 115
5.00	2.26 ± 0.06	312 ± 82

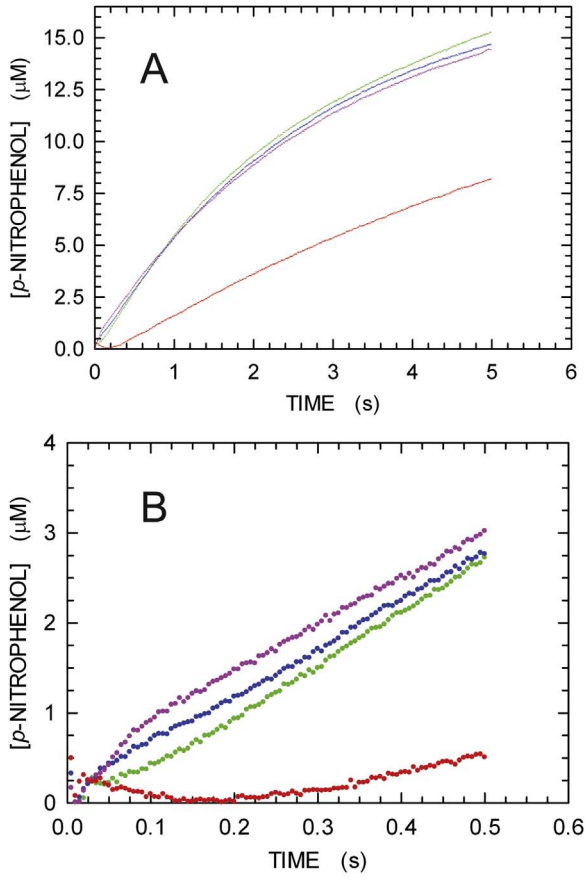

Fig. 3. Pre-steady-state kinetics of *p*-nitrophenyl-β-D-glucopyranoside hydrolysis catalyzed by sweet almond β-glucosidase. (A) Reactions were assayed using 18 mg/mL of crude enzyme and 0.55 mM substrate, in the absence (green dots), or in the presence of 0.125 (blue dots), 0.250 (magenta dots) or 2.5 mM (red dots) imidazole. (B) Detail of the initial phase of reactions reported in Panel A. (For interpretation of the references to color in this figure legend, the reader is referred to the web version of this article).

3.2. Partial purification of β-glucosidase and steady-state activity assays

To better understand whether single or multiple isoforms of β-glucosidase were contributing to the observed activity in the previous assays, the crude enzyme was subjected to gel filtration chromatography, using a Superdex 200 column. The chromatogram accordingly obtained revealed 2 peaks, whose elution volume corresponded to molecular masses equal to 109.6 and 44.8 kDa, respectively (Fig. 4A). Further, the two fractions located at maximal peak amplitude were analyzed by SDS-PAGE and mass spectrometry. Electrophoresis revealed the presence, in the first peak, of two proteins, respectively featuring 63.5 and 45.8 kDa (Fig. 4A). By the same means, we also detected, in the second peak, the 45.8 kDa protein only (Fig. 4A). Using mass spectrometry, we identified both high and low molecular mass proteins as *Prunus dulcis* β-glucosidase (Supplementary Tables 1–3). However, we could not unambiguously locate the truncation of the low

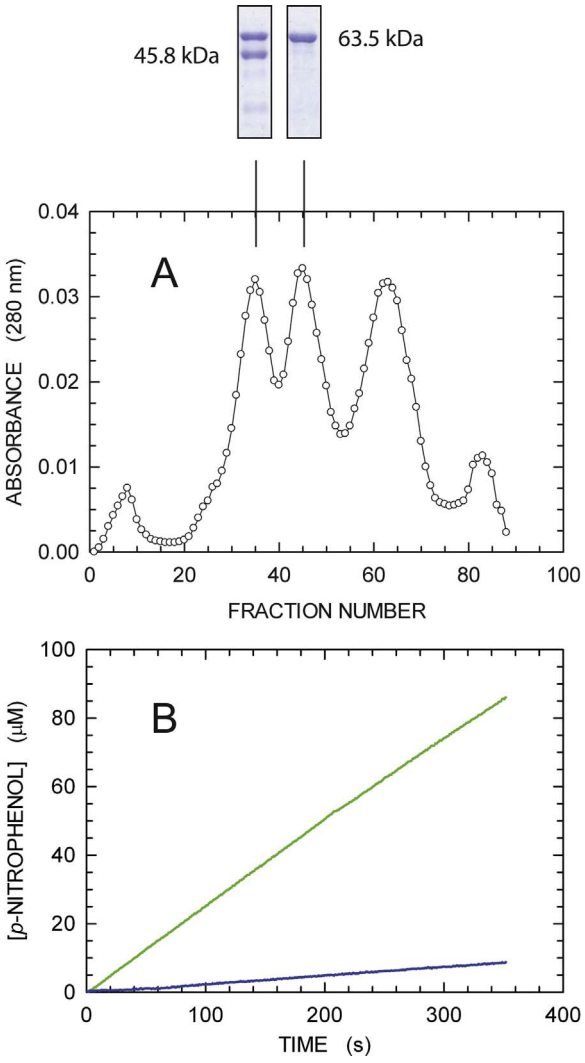

Fig. 4. Partial purification and steady-state kinetic properties of sweet almond β-glucosidase. (A) Gel filtration chromatography of crude enzyme. The SDS-PAGE of fractions 35 and 45 is shown at the top, and the estimated molecular masses of the proteins present in the two major bands are also reported. (B) Time-course of *p*-nitrophenyl-β-D-glucopyranoside hydrolysis catalyzed by dimeric (green dots) or monomeric (blue dots) sweet almond β-glucosidase. Assays were performed at pH 6 using 0.75 mM substrate, in the presence of 60 μg/mL of monomeric or dimeric enzyme.

molecular mass subunit of β-glucosidase dimer (Supplementary Tables 1–3). The activity of both isoforms was then tested in the presence of 1 mM pNPGluc and 60 μg/mL of proteins, and we observed a consistently higher activity exerted by the dimer (Fig. 4B). The initial velocities were indeed determined as 246 ± 0.25 and 25 ± 0.07 nM/s for dimeric and monomeric enzyme, respectively.

3.3. Purification to homogeneity of β-glucosidase

To isolate homogeneous sweet almond β-glucosidase taking advantage of its almost neutral pI (6.03), we first subjected the crude enzyme to anion-exchange chromatography. A consistent fraction of the enzyme, containing both full-length and truncated isoforms, was recovered with the column wash (Fig. 5A). This sample was then concentrated and loaded onto a Superdex 200 column, from which highly purified dimeric and monomeric β-glucosidase were eluted (Fig. 5B–D). The two purified isoforms were finally concentrated, and used to perform activity assays under steady-state and pre-steady-state conditions.

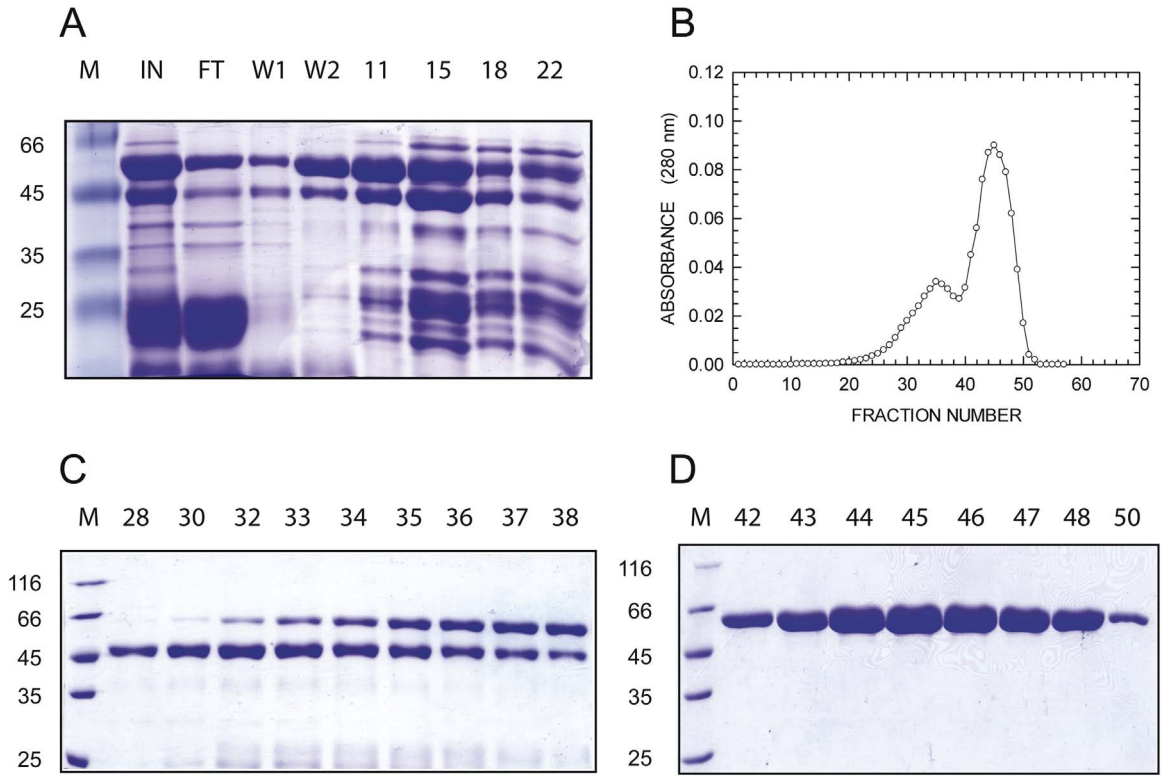

Fig. 5. Purification of sweet almond β-glucosidase. (A) SDS-PAGE of fractions eluted from a Hi-Trap Q anion exchange column, onto which crude enzyme was loaded. M, IN, FT, W1, W2: molecular mass markers, input, flow-through, first column wash, and second column wash, respectively. The electrophoretic pattern of fractions 11, 15, 18, and 22 eluted applying a linear NaCl gradient to the column is also shown. (B) Gel filtration chromatography (Superdex 200 column) of the second wash previously eluted from the Hi-Trap Q ion-exchange column. (C) and (D) SDS-PAGE of fractions eluted from the gel filtration column. M: molecular mass markers.

3.4. Activity assays with homogeneous β-glucosidase

The steady-state activity of purified β-glucosidase was determined using 1 mM pNPGluc in the presence of monomeric (46 nM) or dimeric (7.5 nM) enzyme, respectively. In agreement with the observation obtained with partially purified isoforms, dimeric β-glucosidase performed significantly better than the monomeric counterpart (Fig. 6A), with initial velocities equal to 1.08 ± 0.002 and 0.2 ± 0.00036 μM/s, respectively. The corresponding k_{obs} were accordingly determined as 144 and 4.3 s^{-1} for dimer and monomer, respectively. Very similar observations were obtained under pre-steady-state conditions, with the monomeric enzyme featuring much lower activity when compared with the dimeric isoform (Fig. 6B).

The k_{cat} and K_m of both isoforms of sweet almond β-glucosidase were determined using *p*-nitrophenyl-β-D-glucopyranoside as substrate and 45 nM enzyme (monomer or dimer) at pH 6, in the absence or in the presence of 0.125 mM imidazole. Under these conditions, the dimeric form showed higher activity, featuring V_{max} and K_m equal to 8.26 ± 2.07 μM/s and 2.26 ± 0.06 mM, respectively, while the corresponding constants of the monomeric enzyme were determined as equal to 0.94 ± 0.12 μM/s and 1.64 ± 0.04 mM (Fig. 7A and B, Table 2). According to these data, the k_{cat} of dimeric and monomeric β-glucosidase can be calculated as 184 and 21 s^{-1}, respectively. As expected, imidazole did significantly increase the K_m of both isoforms, i.e. to 6.71 ± 0.14 and 1.93 ± 0.05 mM for dimer and monomer, respectively (Fig. 7A and B, Table 2). On the contrary, imidazole did not significantly alter the V_{max} of both isoforms. In the presence of imidazole, the values of this constant were indeed equal to 20.41 ± 10.61 and 0.86 ± 0.16 μM/s for dimer and monomer, respectively (Fig. 7A and B, Table 2).

To investigate the effect of low concentrations of imidazole towards the pre-steady-state activity of pure isoforms of β-glucosidase, we performed stopped-flow experiments under the same conditions previously used to assay the crude enzyme, i.e. 0.25 or 0.5 mM imidazole eventually added to the syringe containing 2 μM β-glucosidase, and 1.1 mM pNPGluc added to the substrate syringe. Remarkably, when pure dimeric enzyme was assayed, we again observed a transient activation of β-glucosidase exerted by imidazole. In particular, the lag time observed with the crude enzyme in the absence of imidazole was also detected with purified dimer (Fig. 8A and B). This lag time lasted for about 2 s and preceded maximal activity, which obeyed zero-order kinetics for the last 3 s of the time interval considered, and was equal to 5.22 ± 0.08 μM/s. When considering that the final enzyme concentration used in this assay was equal to 1 μM, we estimate k_{obs} equal to 5 s^{-1}. Imidazole was observed to activate dimeric β-glucosidase, although in slightly different modes when compared with those exerted towards the crude enzyme. When 0.25 mM imidazole was used (blue dots), a very short lag phase (< 0.5 s) was detected, followed by zero-order kinetics, which lasted for 2.5 s and accounted for an initial velocity equal to 4.13 ± 0.05 μM/s (Fig. 8A and B). The effect induced by 0.5 mM imidazole (pink dots) towards the dimer was slightly different when compared to the action observed in the presence of crude enzyme. With pure dimeric β-glucosidase the reaction velocity over the initial two seconds was significantly higher when compared with the control (Fig. 8A and B) during the first 2 s, and was subsequently equal to 3.5 ± 0.06 μM/s. However, increasing imidazole concentration from 0.25 to 0.5 mM did not further enhance the initial velocity of the reaction, in contrast with the previous observation obtained in the presence of crude enzyme (cf. Figs. 3 and 8).

When monomeric enzyme was tested under pre-steady-state conditions, imidazole did not trigger any significant effect, neither at 0.25 nor at 0.5 mM (Fig. 8C). Accordingly, both steady-state and pre-steady-state assays indicate monomeric β-glucosidase as relatively insensitive to low imidazole concentrations (Figs. 7A and 8C).

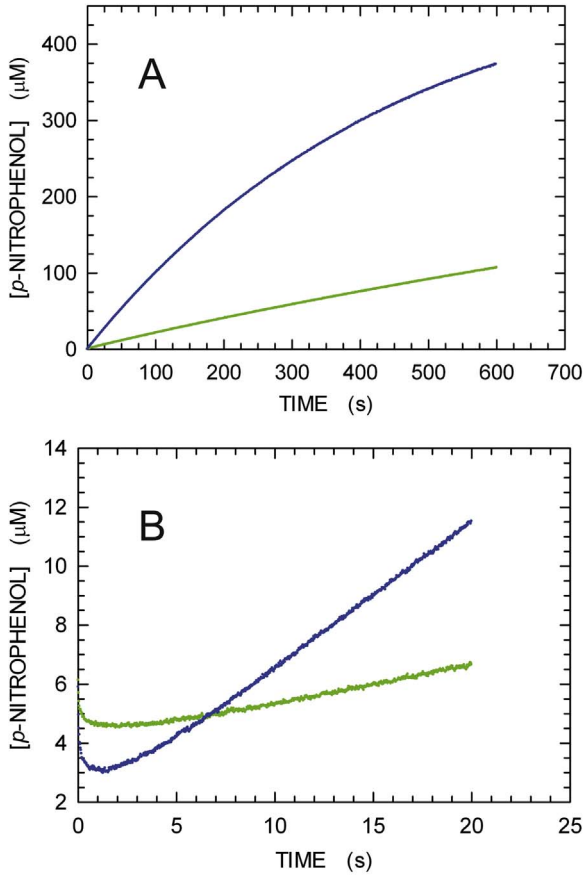

Fig. 6. Steady-state and pre-steady-state kinetics of *p*-nitrophenyl-β-D-glucopyranoside hydrolysis catalyzed by sweet almond β-glucosidase. (A) Steady-state kinetics detected at pH 6 using 0.75 mM substrate, in the presence of 46 nM monomeric (green dots), or 7.5 nM dimeric (blue dots) enzyme. (B) Pre-steady-state kinetics detected at pH 6 using 0.55 mM substrate, in the presence of 260 nM of monomeric (green dots) or dimeric (blue dots) enzyme.

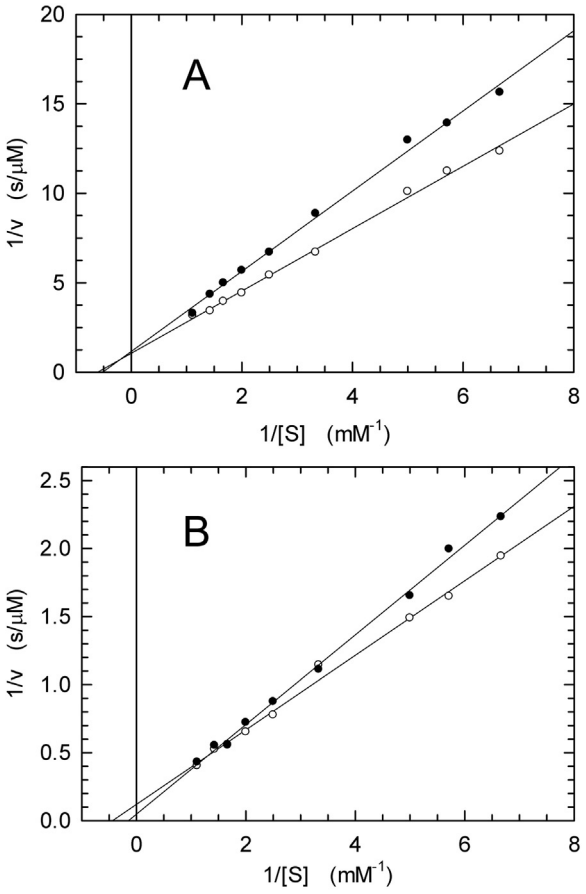

Fig. 7. Lineweaver-Burk plots of *p*-nitrophenyl-β-D-glucopyranoside hydrolysis catalyzed by sweet almond β-glucosidase at pH 6 under steady-state conditions. (A) Initial velocities of reactions catalyzed by 45 nM enzyme monomer, and detected in the absence (empty circles) or in the presence (filled circles) of 0.125 mM imidazole. (B) Initial velocities of reactions catalyzed by 45 nM enzyme dimer, and detected in the absence (empty circles) or in the presence (filled circles) of 0.125 mM imidazole.

4. Discussion

We have shown here that 2 isoforms of sweet almond β-glucosidase can be conveniently purified by ion-exchange and gel filtration chromatography. In particular, we isolated to homogeneity a heterodimer, containing a full-length (62 kDa) and a truncated (46 kDa) subunit, and we also purified a full-length (62 kDa) monomer. The commercial crude enzyme preparation which represented our starting material did not contain a significant amount of homodimeric full-length β-glucosidase. This is apparently in contrast with previous reports, describing the molecular mass of native sweet almond β-glucosidase as equal to 140 ± 20 kDa [22,23]. It is however important to remark that: i) when this homodimer was subjected to SDS-PAGE, two bands were clearly visible; ii) the protein extract used to isolate this enzyme did contain two isoforms, as revealed by native electrophoresis followed by activity staining [22,23]. Of these two isoforms, the purification of only one (the 120 kDa enzyme) was pursued [22,23]. The absence of homodimer in our crude starting material is probably due to a partial processing occurring during fruit development. It was indeed recently reported that during the maturation of fruits, different isoforms of β-glucosidase can be detected, both in sweet and in bitter almonds [24].

The tertiary structure of sweet almond β-glucosidase is unknown. To interpret the kinetic observations reported here, we propose a model of the sweet almond enzyme, obtained using as a template the homologous protein from *Zea mays*, the tertiary structure of which was determined [25]. According to this model, the almond β-glucosidase features α/β TIM barrel conformation (Fig. 9). As expected for this class of proteins, the catalytic E426 residue lies at the C-ter side of the barrel β strands. By searching for residues in proximity of E426, the presence of another glutamate located at the same side of the barrel can be easily identified, i.e. E210. The measured distance between E426 and E210 δ carbons of the almond enzyme is equal to 4.9 Å. In *Zea mays* and *Thermotoga maritima* β-glucosidases, the corresponding distance between the 2 catalytic residues is 4.92, and 5.23 Å, respectively [25,26]. Taking into account that E426 is the nucleophile [5], we propose E210 as the acid/base catalytic glutamate of the sweet almond β-glucosidase. Among the other amino acids relevant for catalysis, our model of the sweet almond enzyme predicts: i) W165, which is located at 4.45 Å from E210 and could be important for the stacking of the substrate aromatic ring, similarly to the role of W378 in the *Zea mays* enzyme; ii) H164, the nitrogens of which are located at 4.5–5 Å from E426, potentially responsible for an interaction with the 3-OH substrate, as H142 does in the *Zea mays* β-glucosidase.

We have shown here that dimeric β-glucosidase is significantly more active than its monomeric counterpart, both under steady-state and pre-steady-state conditions. This observation is in substantial agreement with previous reports, showing that only dimeric β-glucosidases are active, independently of their phylogenetic position [27–29]. Nevertheless, a couple of family 1 β-glucosidases from psychrophilic microorganisms were reported to be catalytically competent in monomeric form [30,31]. The calculated pI values of these cold-adapted β-glucosidases, i.e. 5.05 [30] and 4.98 [31], suggest the absence of an appropriate surface to be engaged in enzyme oligomerization. In the *Zea mays* enzyme, the dimer interface, with the two subunits disposed

Table 2
Sweet almond β-glucosidase kinetic constants determined assaying at pH 6 the activity of 45 nM enzyme (monomer or dimer) in the absence or in the presence of imidazole, and using *p*-nitrophenyl-β-D-glucopyranoside as substrate.

	[Imidazole] (mM)	K_m (mM)	V_{max} (μM/s)	k_{cat} (s^{-1})	k_{cat}/K_m ($mM^{-1}\ s^{-1}$)
Monomer	–	1.64 ± 0.04	0.94 ± 0.12	21	12.8
Monomer	0.125	1.93 ± 0.05	0.86 ± 0.16	19	9.8
Dimer	–	2.26 ± 0.06	8.26 ± 2.07	184	81
Dimer	0.125	6.71 ± 0.14	20.41 ± 10.61	454	68

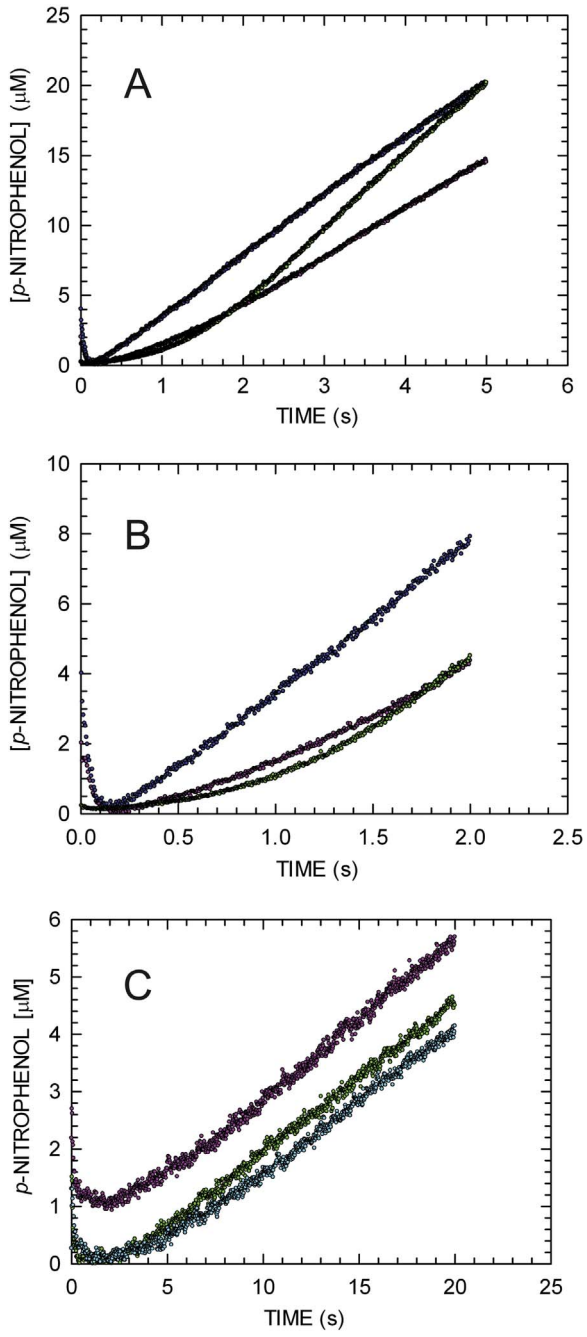

Fig. 8. Pre-steady-state kinetics of *p*-nitrophenyl-β-D-glucopyranoside hydrolysis catalyzed by dimeric and monomeric sweet almond β-glucosidase. (A) Reactions were assayed using 0.95 μM of enzyme dimer and 0.55 mM substrate, in the absence (green dots), or in the presence of 0.125 (blue dots) or 0.250 (magenta dots) mM imidazole. (B) Detail of the initial phase of reactions reported in Panel A. (C) Reactions were assayed using 1 μM of enzyme monomer and 0.55 mM substrate, in the absence (green dots), or in the presence of 0.125 (blue dots) or 0.250 (magenta dots) mM imidazole.

Fig. 9. Structural model of sweet almond β-glucosidase. The tertiary structure of the enzyme was obtained from Swiss-Modeller, using as a template the *Zea mays* homologous β-glucosidase (PDB 1e1e). The two catalytic glutamates, E210 and E426, are shown in blue.

side by side, involves about 6% of the exposed surface monomer [25]. This interface does mainly contain hydrophobic interactions, along with a couple of salt bridges [25]. Notably, we observed that monomeric sweet almond β-glucosidase is eluted earlier than the dimer from an anion-exchange column equilibrated at pH 8 (Fig. 5A). This difference suggests a different conformation of the 2 sweet almond isoforms, in particular concerning the potential self-interaction interface of the monomeric enzyme. This conformational difference could be related to the observation reported here that the catalytic efficiency (k_{cat}/K_m) of sweet almond monomeric β-glucosidase is ca. 6 times lower when compared with the dimeric isoform (Table 2).

The activation of sweet almond β-glucosidase by imidazole, as reported here, is unexpected. Besides featuring properties of competitive inhibitor at high concentrations (1–5 mM), imidazole was indeed found to activate the enzyme when present at concentrations equalling 0.25 times that of substrate, and exceeding by about two orders of magnitude the enzyme concentration. A similar observation was reported for imidazole derivatives, acting towards histamine methyltransferase as inhibitors or activators at high (mM) and low (μM) concentrations, respectively [32]. In particular, we were able to detect the activation by imidazole of dimeric enzyme under pre-steady-state conditions. In these assays, and in the absence of imidazole, we clearly observed a lag-time before β-glucosidase entered maximal activity. This lag-time, lasting for about 2–3 s, corresponded to the generation of 10 μM p-nitrophenol, which means 10 times the final concentration of enzyme in the observation cell of the stopped flow (Fig. 8). On the contrary, the addition of 0.25 mM imidazole to the enzyme syringe of the instrument (containing 2 μM β-glucosidase) did shorten the lag-time to less than half a second, after which zero-order kinetics was immediately reached, and the generation of about 20 μM product was observed (Fig. 8). We propose that the imidazole can primarily bind to a second site, different from the substrate pocket responsible for compe-

titive inhibition. The binding of imidazole to this alternative site could trigger a conformational change, switching the enzyme from a less to a more proficient catalyst. Subsequently, however, the velocity of the reaction observed in the absence of imidazole gets higher, suggesting that imidazole starts to bind at the active site. Remarkably, isofagomine, a very potent inhibitor of β-glucosidases (featuring K_i values in the nM domain), was shown to slowly bind and inhibit both the *Thermotoga maritima* and the sweet almond enzyme [26,33]. This slow binding and onset of inhibition was attributed to a slow conformational change of the enzyme, converted to a form featuring high affinity for the inhibitior [26,34,35]. It is important to note that this slow binding/inhibiton of isofagomine takes place in the presence of substrate. The binding of imidazole to sweet almond β-glucosidase is most likely slow, and we accordingly decided to add imidazole to the enzyme before the substrate in stopped-flow experiments. This strategy does indeed let to observe the effects of imidazole on reaction kinetics in the presence of enzyme previously converted to an alternative conformation induced by the activator/inhibitor.

The observations reported here indicate that imidazole can act both as competitive inhibitor and activator of β-glucosidases. This dual role of imidazole is most likely linked to conformational transitions of the target enzyme. It will be accordingly of interest to analyze conformational changes of the sweet almond β-glucosidase triggered by imidazole, e.g. by determining fluorescence changes of enzyme tryptophan(s) related to the binding of imidazole. It is our hope that similar studies will contribute to a better understanding of the mechanisms involved in activation/inhibition of glycohydrolases.

Acknowledgments

The Authors are indebted to Mike Repasky (KinTek Corporation, Snow Shoe, PA 16874, USA) and to Salvatore Spatola, Fabrizio Galloni, and Matteo Marano (University of Bologna) for the outstanding assistance in setting up the KinTek SF2004 stopped-flow.

Appendix A. Supplementary material

Supplementary data associated with this article can be found in the online version at doi:10.1016/j.bbrep.2017.03.007.

References

[1] D.E. Koshland, Stereochemistry and mechanism of enzymatic reactions, Biol. Rev. 28 (1953) 416–436.
[2] F.W. Dahlquist, T. Rand-Meir, M.A. Raftery, Application of secondary α-deuterium kinetic isotope effects to studies on enzyme catalysis. Glycoside hydrolysis by lysozyme and β-glucosidase, Biochemistry 8 (1969) 4214–4221.
[3] S.G. Withers, R. Aebersold, Approaches to labeling and identification of active site residues in glycosidases, Prot. Sci. 4 (1995) 361–372.
[4] D.L. Zechel, S.G. Withers, Glycosidase mechanisms: anatomy of a finely tuned catalyst, Acc. Chem. Res. 33 (2000) 11–18.
[5] S. He, S.G. Withers, Assignment of sweet almond β-glucosidase as a family 1 glucosidase and identification of its active site nucleophile, J. Biol. Chem. 272 (1997) 24864–24867.
[6] C.S. Hudson, H.S. Paine, The hydrolysis of salicin by the enzyme emulsin, J. Am. Chem. Soc. 31 (1909) 1242–1248.
[7] M.P. Dale, H.E. Ensley, K. Kern, K.A.R. Sastry, L.D. Byers, Reversible inhibitors of β-glucosidase, Biochemistry 24 (1985) 3530–3539.
[8] D.E. Eveleigh, A.S. Perlin, A proton magnetic resonance study of the anomeric species produced by D-glycosidases, Carbohydr. Res. 10 (1969) 87–95.
[9] M. Xie, L.D. Byers, Solvent and α-secondary kinetic isotope effects on β-glucosidase, Biochim. Biophys. Acta 1854 (2015) 1776–1781.
[10] M.P. Dale, W.P. Kopfler, I. Chait, L.D. Byers, β-glucosidase: substrate, solvent, and viscosity variation as probes of the rate-limiting steps, Biochemistry 25 (1986) 2522–2529.
[11] A. Wisemann, Fungal and other β-D-glucosidases – their properties and applications, Enzym. Microb. Technol. 4 (1982) 73–78.
[12] E.M. Bowers, L.O. Ragland, L.D. Byers, Salt effects on β-glucosidase: pH-profile narrowing, Biochim. Biophys. Acta 1772 (2007) 1500–1507.
[13] R.L. Nath, H.N. Rydon, The influence of structure on the hydrolysis of substituted phenyl β-D-glucosides by emulsin, Biochem. J. 57 (1954) 1–10.
[14] N.W. Barton, F.S. Furbish, G.J. Murray, M. Garfield, R.O. Brady, Therapeutic response to intravenous infusions of glucocerebrosidase in a patient with Gaucher disease, Proc. Natl. Acad. Sci. USA 87 (1990) 1913–1916.
[15] Y.K. Li, L.D. Byers, Inhibition of β-glucosidase by imidazoles, Biochim. Biophys. Acta 999 (1989) 227–232.
[16] R.A. Field, A.H. Haines, E.J.T. Chrystal, M.C. Luszniak, Histidines, histamines and imidazoles as glycosidase inhibitors, Biochem. J. 274 (1991) 885–889.
[17] H. Hettkamp, G. Legler, E. Bause, Purification by affinity chromatography of glucosidase I, an endoplasmic reticulum hydrolase involved in the processing of asparagine-linked oligosaccharides, Eur. J. Biochem. 142 (1984) 85–90.
[18] G. Cheron, G. Noat, J. Ricard, Hysteresis of plant cell-wall β-glucosidase, Biochem. J. 269 (1990) 389–392.
[19] K.J. Ellis, J.F. Morrison, Buffers of constant ionic strength for studying pH-dependent processes, Methods Enzymol. 87 (1982) 405–426.
[20] M.M. Bradford, A rapid and sensitive method for the quantitation of microgram quantities of protein utilizing the principle of protein-dye binding, Anal. Biochem. 72 (1976) 248–254.
[21] E. Conte, G. Vincelli, R.M. Schaaper, D. Bressanin, A. Stefan, F. Dal Piaz, A. Hochkoeppler, Stabilization of the *Escherichia coli* DNA polymerase III ε subunit by the θ subunit favors *in vivo* assembly of the Pol III catalytic core, Arch. Biochem. Biophys. 523 (2012) 135–143.
[22] P. Lalégerie, La β-glucosidase de l'amande douce (*Amygdalus communis* L.). I. Isolement et purification, Biochimie 56 (1974) 1163–1172.
[23] P. Lalégerie, La β-glucosidase de l'amande douce (*Amygdalus communis* L.). II. Propriétés catalitiques, Biochimie 56 (1974) 1297–1303.
[24] R. Sánchez-Pérez, F.S. Belmonte, J. Borch, F. Dicenta, B.L. Møller, K. Jørgensen, Prunasin hydrolases during fruit development in sweet and bitter almonds, Plant Physiol. 158 (2012) 1916–1932.
[25] M. Czjzek, M. Cicek, V. Zamboni, W.P. Burmeister, D.R. Bevans, B. Henrissat, A. Esen, Crystal structure of a monocotyledon (maize ZMGlu1) β-glucosidase and a model of its complex with *p*-nitrophenyl β-D-thioglucoside, Biochem. J. 354 (2001) 37–46.
[26] D.L. Zechel, A.B. Boraston, T. Gloster, C.M. Boraston, J.M. MacDonald, D.M.G. Tilbrook, R.V. Stick, G.J. Davies, Iminosugar glycosidase inhibitors: structural and thermodynamic dissection of the binding of isofagomine and 1-deoxynojirimycin to β-glucosidases, J. Am. Chem. Soc. 125 (2003) 14313–14323.
[27] B. Henrissat, G.J. Davies, Structural and sequence-based classification of glycoside hydrolases, Curr. Opin. Struct. Biol. 7 (1997) 637–644.
[28] B. Henrissat, I. Callebaut, S. Fabrega, P. Lehn, J.P. Mornon, G.J. Davies, Conserved catalytic machinery and the prediction of a common fold for several families of glycosyl hydrolases, Proc. Natl. Acad. Sci. USA 92 (1995) 7090–7094.
[29] J. Jenkins, L. Lo Leggio, G. Harris, R. Pickersgill, β-glucosidase, β-galactosidase, family A cellulases, family F xylanases and two conserved glutamates near the carboxy-terminal ends of β-strands four and seven, FEBS Lett. 362 (1995) 281–285.
[30] A. Wierzbicka-Wós, P. Bartasun, H. Cieśliński, J. Kur, Cloning and characterization of a novel cold-active glycoside hydrolase family 1 enzyme with β-glucosidase, β-fucosidase and β-galactosidase activities, BMC Biotechnol. 13 (2013) 22.
[31] H.X. Fan, L.L. Miao, Y. Liu, H.C. Liu, Z.P. Liu, Gene cloning and characterization of a cold-adapted β-glucosidase belonging to glycoside hydrolase family 1 from a psychrotolerant bacterium *Micrococcus antarcticus*, Enzym. Microb. Technol. 49 (2011) 94–99.
[32] H. Barth, W. Lorenz, Structural requirements of imidazole compounds to be inhibitors or activators of histamine methyltransferase: investigation of histamine analogues and H_2-receptor antagonists, Agents Actions 8 (1978) 359–365.
[33] A. Lohse, T. Hardlei, A. Jensen, I.W. Plesner, M. Bols, Investigation of the slow inhibition of almond β-glucosidase and yeast isomaltase by 1-azasugar inhibitors: evidence for the 'direct binding' model, Biochem. J. 349 (2000) 211–215.
[34] A. Tanaka, M. Ito, K. Hiromi, Equilibrium and kinetic studies on the binding of gluconolactone to almond β-glucosidase in the absence and presence of glucose, J. Biochem. 100 (1986) 1379–1385.
[35] G. Legler, Glycoside hydrolases: mechanistic information from studies with reversible and irreversible inhibitors, Adv. Carbohydr. Chem. Biochem. 48 (1990) 319–384.